Substrate-Dependent Shift of Optimum pH in Porcine Pancreatic α-Amylase-Catalyzed Reactions

Kazuhiko Ishikawa,* Ikuo Matsui, and Koichi Honda

National Chemical Laboratory for Industry, Higashi 1-1, Tsukuba, Ibaraki 305, Japan

Hiroshi Nakatani

Department of Food Science and Technology, Faculty of Agriculture, Kyoto University, Kyoto 606, Japan

Received November 30, 1989; Revised Manuscript Received March 13, 1990

ABSTRACT: Porcine pancreatic α-amylase (EC 3.2.1.1, abbreviated as PPA) hydrolyzes α-D-(1,4) glucosidic bonds in starch and amylose at random, and the optimum pH for the substrates is 6.9. The optimum pH, however, shifted to 5.2 for the hydrolytic reaction of low molecular weight oligosaccharide substrates such as *p*-nitrophenyl α-D-maltoside, γ-cyclodextrin, maltotetraitol, and maltopentaitol. The optimum pH for the oligosaccharides consisting of more than five glucose residues, such as maltopentaose and maltohexaitol, was 6.9. From the analysis of the hydrolysates, it was clear that the shift of the optimum pH occurred only when the fifth subsite of PPA in the productive binding modes was occupied by a glucosyl residue of the substrates. The value of K_m was independent of pH between 4 and 10 but that of k_{cat} was dependent on pH. The pH profiles of k_{cat} for the above substrates did not fit a simple bell-shaped curve predicted by a two-catalytic-group mechanism. Instead, they were well analyzed theoretically by three pK values and two intrinsic k_{cat} values. Enthalpy changes for the three pK's (4.90, 5.35, and 8.55 at 30 °C) were determined from the temperature dependence of pH profiles for maltopentaitol and maltohexaitol to be 0.0, 2.87, and 7.33 kcal/mol, respectively. These results indicate that productive binding modes of the substrates directly affect the catalytic function of the enzyme. From the present thermodynamic analysis and reported three-dimensional structure at the active site of PPA [Buisson, G. (1987) *EMBO J. 6*, 3909–3916], one can assume that a histidyl residue (101, 201, or 299) acts as a proton donor and two carboxyl groups (Asp 197, Glu 233, or Asp 300) act as proton donors or acceptors, and the productive binding mode covering the fifth subsite changes configurations between the catalytic residues and the glucosidic bond hydrolyzed and modulates kinetic parameters depending on pH.

Porcine pancreatic α-amylase (EC 3.2.1.1, abbreviated as PPA[1]) (MW = 52000) is an endo-type amylase that contains five subsites and catalyzes the random hydrolysis of α-D-(1,4) glucosidic bonds in starch and amylose (Robyt & French, 1970a; Prodanov et al., 1984). Two isozymes (PPA I and II) are known for PPA (Marchis-Mouren & Pasero, 1967). They have the same molecular weight and the same optimum pH for activity but differ slightly in amino acid composition and isoelectric point (Pasero et al., 1981; Kluh, 1981). From the primary structure (Pasero et al., 1986) and crystal structure with 2.9-Å resolution (Buisson et al., 1987), the catalytic residues of PPA I were proposed to be the carboxyl groups of Asp 197 and Asp 300. PPA I resembles Taka amylase A (TAA), a fungal amylase produced by *Aspergillus oryzae*, in terms of the crystal structure and sequence homology around the active site (Matsuura et al., 1984). Unlike TAA, PPA I is activated by chloride ion, which binds to the catalytic site (Buisson et al., 1987; Wakim et al., 1969). The optimum pH's of PPA I and TAA for the hydrolysis of soluble starch and amylose are 6.9 (Wakim et al., 1969) and 5.5 (Matsubara et al., 1959), respectively. Two carboxyl residues are speculated to be the catalytic residues in both enzymes (Matsuura et al., 1984). However, the pH profile of the rate parameter for PPA is not a simple bell-shaped curve expected from the two-catalytic-residue mechanism. Therefore, it is important to obtain information on catalytic residues from kinetic analysis of enzyme actions. The values of pK's and enthalpy changes can indicate probable catalytic amino acid residues. For the analysis of pH profiles, small substrates with only one possible cleavage site are useful because the complexity of "multiple attack" action (Robyt & French, 1967, 1970b) on amylose and starch and other effects due to different productive binding modes (Robyt & French, 1970a) may be eliminated.

In this paper, we report the detailed analysis of pH profiles of PPA by using low molecular substrates and the probable amino acid residues related to the catalysis function determined from thermodynamic data.

Materials and Methods

Materials. PPA was purified in the crystalline state from porcine pancreatin purchased from Sigma Chemical Co., as described by Loyter and Shramm (1962). TSK-Gel DEAE Toyopearl 650 S and TSK-G-2000 PW columns (7.5 × 600 mm i.d.) were purchased from Toyo Soda Manufacturing Co., Ltd. *p*-Nitrophenyl α-D-maltoside (G2-PNP) was purchased from Calbiochem Corp. Soluble starch, amylose A (MW = 2900), maltotetraose (G4), maltopentaose (G5), maltohexaose (G6), and γ-cyclodextrin (γ-CD) were purchased from Nacalai Tesque Ltd. Maltotetraitol (G4OH), maltopentaitol (G5OH), and maltohexaitol (G6OH) were prepared by the reduction of G4, G5, and G6 with sodium borohydride ac-

[1] Abbreviations: PPA, porcine pancreatic α-amylase; TAA, Taka amylase A; γ-CD, γ-cyclodextrin; G, glucose; G2, maltose; G3, maltotriose; G4, maltotetraose; G5, maltopentaose; G6, maltohexaose, G2OH, maltitol; G3OH, maltotriitol; G4OH, maltotetraitol; G5OH, maltopentaitol; G6OH, maltohexaitol; TNS, 2-*p*-toluidinylnaphthalene-6-sulfonate.

0006-2960/90/0429-7119$02.50/0

cording to the method of Walfolm and Thompson (1963). Other chemicals were of commercial guaranteed or reagent grade.

Purification of PPA I. PPA I was separated from the crystalline preparation of PPA by using TSK-Gel DEAE Toyopearl 650 S (Sakano et al., 1983). The crystalline preparation purified from pancreatin was dialyzed against 20 mM Tris-HCl buffer (pH 8.3) containing 1 mM $CaCl_2$ and applied on the TSK-Gel DEAE Toyopearl column buffered with the same buffer. Only PPA I was eluted from this column. PPA II was adsorbed. The combined fractions of PPA I that showed a single band on polyacrylamide gel electrophoresis (pH 9.0) (Davis, 1964) were dialyzed against 25 mM phosphate buffer (pH 6.9) containing 30 mM NaCl, 1 mM $CaCl_2$, and 0.02% NaN_3 and stored at 4 °C. (PPA I is abbreviated as PPA.)

Enzyme Assay. The hydrolytic reaction was initiated by mixing a PPA solution with a substrate solution in a 25 mM Tris–acetate buffer (pH 3.5–9.0) or in a 25 mM borate–NaOH buffer (pH 9.0–11.0), containing 30 mM NaCl and 1 mM $CaCl_2$ at 30 °C. The reactions for soluble starch, amylose, and the oligosaccharides (G5, G4OH, G5OH, and G6OH) were terminated by the addition of the same volume of 0.08 N NaOH solution. The activities for the substrates were determined by reductometry; for soluble starch and amylose the modified Nelson–Somogyi method (Hiromi et al., 1963) was used, and for the oligosaccharides the method of Dygert et al. (1965) was used. For G2-PNP, the reaction was terminated by pouring 0.5 mL of the reaction mixture into 1 mL of the 0.01 N NaOH solution, and the activity was measured by the 400-nm absorption of the product *p*-nitrophenol liberated within 2 min. The alkaline hydrolysis of G2-PNP was negligible. The hydrolysis of γ-CD was determined by utilizing the fluorescence of 2-*p*-toluidinylnaphthalene-6-sulfonate (TNS) (Kondo et al., 1976). Since the fluorescence emission (450 nm) of TNS excited at 366 nm is increased by the addition of CD, the amount of γ-CD is measurable from the increment of the fluorescence emission at 450 nm.

The molarity of PPA was determined from the absorbance at 280 nm on the basis of a molecular weight of 52 000 and $A^{1\%} = 24.0$ (Elodi, 1972).

The kinetic parameters (k_{cat} and K_m) were determined by the nonlinear least-squares method with the Taylor expansion (Sakoda & Hiromi, 1976). In some cases, k_{cat} was determined under conditions where the substrate concentration was much greater than K_m.

Analysis of the Products. Analysis of oligosaccharides was carried out by using a TSK-G-2000 PW column with the JASCO Trirotar-III high-performance liquid chromatography (HPLC) apparatus equipped with a differential refractometer (Ishikawa & Hirata, 1989). Elution was performed with distilled water at a flow rate of 1 mL/min.

Results

Hydrolysis of Amylose and Soluble Starch. The pH profile for the hydrolytic activity of PPA for amylose A (MW = 2900) showed that the optimum pH is 6.9. A similar profile was obtained with soluble starch, and the optimum pH of 6.9 was confirmed as reported by Wakim et al. (1969). However, the pH profiles of PPA for these substrates do not reflect exactly the initial hydrolytic activity for the cleavage of their α-(1,4) glucosidic bonds because the multiple attack action of PPA on these long-chain substrates depends on pH (Robyt & French, 1967; Kondo et al., 1978). Therefore, we used oligosaccharide conjugates with sorbitol and *p*-nitrophenol and

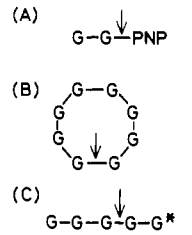

FIGURE 1: Hydrolytic patterns of G2-PNP (A), γ-CD (B), and G5 (C). Glucose residues, the reducing end of the oligosaccharide, *p*-nitrophenol, and α-(1,4) glucosidic bonds are shown as G, *, PNP, and –. The bonds cleavable by PPA are shown by arrows.

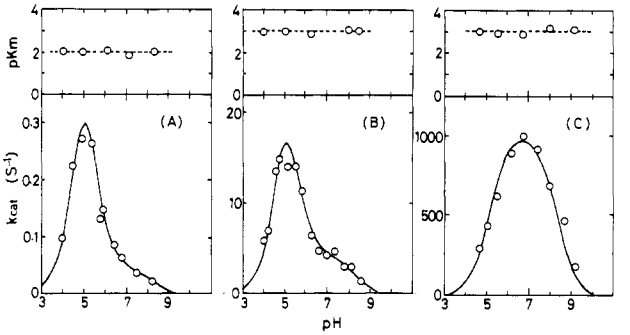

FIGURE 2: Effect of pH on the K_m and k_{cat} of the hydrolytic reaction of G2-PNP (A), γ-CD (B), and G5 (C). The theoretical curves fitting these data were calculated by using eq 1 and the estimated parameters $pK_1 = 4.90$, $pK_2 = 5.35$, and $pK_3 = 8.55$ and (A) $k_1 = 0.608$ s^{-1} and $k_2 = 0.040$ s^{-1}, (B) $k_1 = 32.6$ s^{-1} and $k_2 = 4.2$ s^{-1}, and (C) $k_1 = 368$ s^{-1} and $k_2 = 1010$ s^{-1}.

γ-CD as substrates to analyze pH profiles without multiple attack action.

Hydrolysis of G2-PNP. G2-PNP is favorable to study the hydrolytic activity of PPA, since it is the smallest substrate that can be hydrolyzed at one position, shown in Figure 1A, to give *p*-nitrophenol (Levitzki & Steer, 1974). The increase of the 400-nm absorbance due to the liberated *p*-nitrophenol was linear within 10% conversion. The initial rate of hydrolysis was obtained from the slope of the linear plot. The optimum pH of the rate constant (k_{cat}) for G2-PNP was 5.2, unlike that for soluble starch and amylose, and the value of the Michaelis constant (K_m) was 5.0 mM over the entire pH range examined (Figure 2A). Furthermore, the pH profile of k_{cat} deviates at around pH 7 from the theoretical profile based on the two-ionizing-group catalysis mechanism (Dixon et al., 1979).

Hydrolysis of γ-CD. γ-CD was hydrolyzed at the one cleavage position in the cyclic α-(1,4) glucosidic bonds (Figure 1B) to linear maltooctanoside, which was then decomposed to smaller oligosaccharides by the multiple attack action of PPA (Abdullah et al., 1966). Thus, the decreased rate of γ-CD hydrolysis measured by the TNS fluorescence method reflects directly the initial hydrolysis rate for γ-CD within 10–20% conversion. The optimum pH of the k_{cat} for γ-CD was 5.2, in accord with that for G2-PNP, and the value of K_m was also independent of pH (Figure 2B). This pH profile also shows deviation at around pH 7 from the theoretical curve obtained by assuming two catalytic groups.

Hydrolysis of G5, G4OH, G5OH, and G6OH. For G5, the hydrolysis occurred at one cleavage position without multiple attack (Figure 1C) as reported by Robyt and French (1970a) in the pH 4.0–9.3 region (presented at the annual meeting of the Agriculture Chemical Society of Japan in 1989). The initial hydrolysis rate was calculated from the slope of the linear time course plot obtained with reductometry within 10–20% conversion. The optimum pH of k_{cat} was 6.9, identical with those for soluble starch and amylose, and the value of

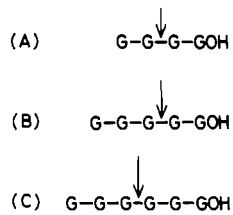

FIGURE 3: Hydrolytic patterns of G4OH (A), G5OH (B), and G6OH (C). G*n*OH indicates the reduced oligosaccharide obtained with sodium borohydride from G*n*. The bonds cleavable by PPA are shown by arrows.

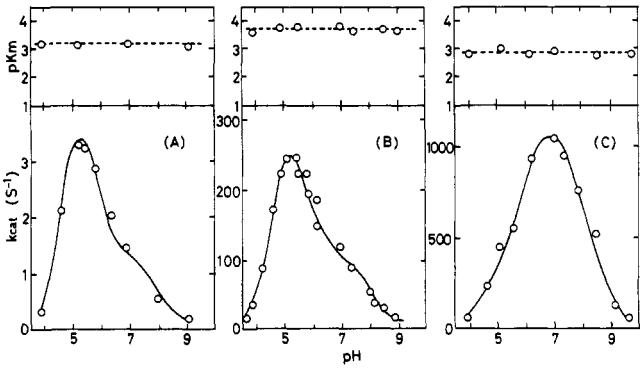

FIGURE 4: Effect of pH on the K_m and k_{cat} of the hydrolytic reaction of G4OH (A), G5OH (B), and G6OH (C). The theoretical curves fitting these data were calculated by using eq 1 and the estimated parameters $pK_1 = 4.90$, $pK_2 = 5.35$, and $pK_3 = 8.55$ and (A) $k_1 = 6.23\ s^{-1}$ and $k_2 = 1.47\ s^{-1}$, (B) $k_1 = 490\ s^{-1}$ and $k_2 = 98\ s^{-1}$, and (C) $k_1 = 482\ s^{-1}$ and $k_2 = 912\ s^{-1}$.

K_m was independent of the pH examined (Figure 2C).

Next, we used some substrates without a reducing end, G4OH, G5OH, and G6OH, to measure the initial rate of hydrolysis of the α-D-(1,4) glucosidic bond at 10, 20, 30, and 37 °C by the reductometric method. For these substrates, the initial rate of hydrolysis of the α-D-(1,4) glucosidic bond could be measured accurately from the reductometric determination because there was no reducing end. The hydrolysates from these substrates were analyzed by HPLC, although reduced oligosaccharides (G*n*OH) were not separated from the corresponding oligosaccharides with reducing ends (G*n*). In the case of G4OH, the products G2 and G2OH appeared at the same position. Similarly, the products from G6OH were G3 and G3OH, which also eluted as one peak. In the case of G5OH, two peaks at the positions of G2 and G3 were detected. The analysis of the products from G5OH with paper chromatography indicated that they were G2OH and G3, since the product at the G3 position had a reducing end but that at G2 did not. The product analysis proved that these substrates were hydrolyzed at a single cleavage site shown in Figure 3, regardless of the pH, substrate concentration, and reaction temperature examined. The K_m values for the substrates were invariable in the range of pH 4–10. The k_{cat} values strongly depended on the pH, and the optimum pH for the hydrolysis of G4OH and G5OH was 5.2 (Figure 4, panels A and B), whereas that for G6OH was 6.9 (Figure 4, panel C).

Discussion

The optimum pH for the hydrolytic activity of PPA under physiological conditions has long been believed to be around neutrality on the basis of the study on soluble starch and amylose (Wakim et al., 1969). However, we found that it shifts to 5.2 in the case of some low molecular weight substrates (Figure 2) and that the shift depends on the occupancy

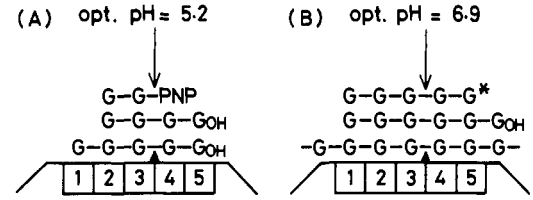

FIGURE 5: Schematic representation of the active site of PPA and the productive binding mode of substrates. Subsites per glucose residue (G) of the substrates are numbered 1–5 from the nonreducing end. The catalytic residue is located between subsites 3 and 4. (A) Productive binding modes of G2-PNP, G4OH, and G5OH. Optimum pH of the hydrolytic activity is 5.2. (B) Productive binding modes of G5, G6OH, and amylose. Optimum pH of the hydrolytic activity is 6.9.

Scheme I[a]

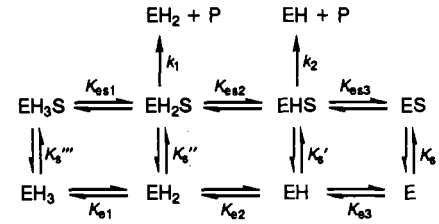

[a] E = enzyme (PPA); S = substrate; P = product; H = proton.

of one enzyme subsite critical for the difference of only one glucose residue in the substrates (Figure 4). Analysis of the products from the substrates G4OH–G6OH indicates that the shift of the optimum pH from 6.9 to 5.2 occurs when subsite 5 of PPA is not occupied by a glucose residue of the substrate in the productive binding mode (Figure 3). This rule holds also for the other substrates (amylose, starch, G5, and G2-PNP), as shown in Figure 5. The optimum pH for γ-CD is 5.2, suggesting that subsite 5 is not occupied in the productive binding mode.

If there are two catalytic ionization groups, the pH profiles must be bell-shaped and the optimum pH should be substrate-independent like TAA, because the fact that the K_m values of PPA are independent of pH indicates that the pK values of the ionization groups contributing to the catalytic function of PPA are substrate-independent. Actually, PPA is showing a substrate-dependent shift of the optimum pH without any change in the pK values of the catalytic groups. The substrate-dependent shift of the optimum pH, the pH-independent K_m, and the deviation of pH profiles from the theoretical curves based on the contribution of two ionizing groups to the catalytic activity (G2-PNP, γ-CD, G4OH, and G5OH) led to the modified reaction mechanism with three ionization groups shown in Scheme I.

In Scheme I, we assume that three ionization groups contribute to the enzyme activity. K_{e1}, K_{e2}, and K_{e3} are the ionization constants of the enzyme at the first, second, and third ionization stages, respectively, and K_{es1}, K_{es2}, and K_{es3} are those of the enzyme–substrate complexes. K_s, K_s', K_s'', and K_s''' are the dissociation constants between the substrate and the enzyme in the successive ionized states E, EH, EH_2, and EH_3, respectively. Hydrolysis of the substrates occurs only from the complex EH_2S and EHS with the rate constants k_1 and k_2, respectively. The relative values of k_1 and k_2 determine the apparent optimum pH of the hydrolysis. When the substrate is large enough to occupy subsite 5 of PPA, the complex EHS is more active than the complex EH_2S; the k_2 value is greatly increased and the optimum pH shifts toward neutrality. Thus, the substrate-dependent shift of the optimum pH observed for the hydrolytic activity of PPA can be explained quantitatively by Scheme I.

Table I: Kinetic Parameters Computed from the Data of k_{cat} for G5OH and G6OH[a]

parameter	substrate	
	G5OH	G6OH
pK_1	4.90 ± 0.05	
pK_2	5.35 ± 0.06	
pK_3	8.55 ± 0.02	
ΔH_1 (kcal/mol)	0.0 ± 0.07	
ΔH_2 (kcal/mol)	2.87 ± 0.12	
ΔH_3 (kcal/mol)	7.33 ± 0.10	
k_1 (s^{-1})	490 ± 37	482 ± 30
k_2 (s^{-1})	98 ± 3.8	912 ± 14
E_1 (kcal/mol)	19.7 ± 0.66	19.5 ± 1.3
E_2 (kcal/mol)	20.1 ± 1.1	18.8 ± 0.26

[a] The 14 kinetic parameters on the activity of PPA including their standard errors were obtained from the k_{cat} values at the different pH and temperature by using eqs 1 and 2 and a nonlinear least-squares method with Gauss–Newton variations. The values of pK_{1-3} and k_{1-2} were those at 30 °C.

The fact that K_m is independent of pH allows us to assume $K_s = K_s' = K_s'' = K_s'''$, $K_{e1} = K_{es1}$, $K_{e2} = K_{es2}$, and $K_{e3} = K_{es3}$. Then, the following rate equation (eq 1) can be derived from Scheme I by use of the stationary state method.

$$k_{cat} = \frac{k_1}{\frac{K_{e2}K_{e3}}{H^2} + \frac{K_{e2}}{H} + 1 + \frac{H}{K_{e1}}} + \frac{k_2}{\frac{K_{e3}}{H} + 1 + \frac{H}{K_{e2}} + \frac{H^2}{K_{e1}K_{e2}}} \quad (1)$$

Here K_{e1}, K_{e2}, K_{e3}, k_1, and k_2 are functions of temperature as shown:

$$pK_{1-3} = -\log K_{e1-3}$$

$$\Delta H_{1-3} = 2.3R\frac{d(pK_{1-3})}{d(1/T)}$$

$$E_{1-2} = -R\frac{d \ln k_{1-2}}{d(1/T)} \quad (2)$$

Here ΔH_1, ΔH_2, and ΔH_3 are enthalpy changes for pK_1, pK_2, and pK_3, E_1 and E_2 are activation energies for k_1 and k_2, and R and T are the gas constant and temperature, respectively.

The kinetic constants and their standard errors can be calculated by using eqs 1 and 2 and a nonlinear least-squares method "program system SALS" with Gauss–Newton variation (Nakagawa & Oyanagi, 1982). The rate parameters pK_1, pK_2, pK_3, k_1, and k_2, the enthalpy changes for pK_1, pK_2, and pK_3, and the activation energies for k_1 and k_2 are determined most accurately by using the pH profile data for G6OH and G5OH at 10–37 °C since they are the substrates with different optimum pH's and rather small differences between their k_1 and k_2 values. The values of pK_1, pK_2, and pK_3, based on the dissociation constants of the free enzyme itself, are independent of substrates. Therefore, we must obtain the following 14 parameters, pK_1, pK_2, pK_3, ΔH_1, ΔH_2, ΔH_3, and k_1, k_2, E_1, and E_2 for G5OH and G6OH, from the temperature-dependent pH profile data for G5OH and G6OH at 10, 20, 30, and 37 °C by using eq 1 in which eq 2 is substituted. As a result of the computer analysis of the pH profiles, we obtained the above parameters for G5OH and G6OH shown in Table I. The experimental data and theoretical line computed from eqs 1 and 2 with the parameters (Table I) are shown in Figure 6. The values of k_1 and k_2 for other substrates at 30 °C can be determined by using these same values of pK_{1-3}. As shown in Figures 2 and 4, theoretical curves (solid lines) (values of

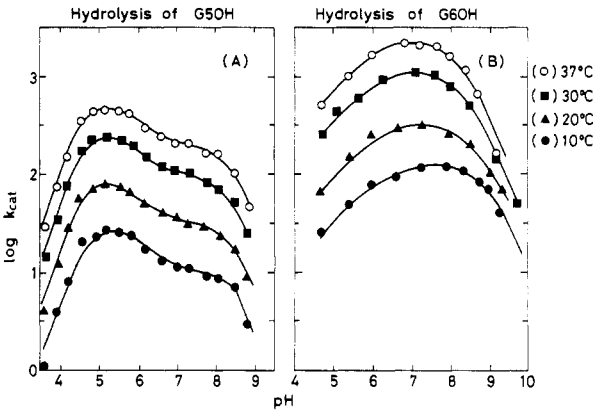

FIGURE 6: Effect of temperature on pH profiles of k_{cat} for G5OH (A) and G6OH (B). The experimental points (●, 10 °C; ▲, 20 °C; ■, 30 °C; and ○, 37 °C) were determined at substrate concentrations much greater than the value of K_m. The theoretical curves fitting these data were calculated by using eqs 1 and 2 and the parameters estimated (Table I).

pK_1, pK_2, pK_3, k_1, and k_2 are described in the figure legends) fit in well with the experimental values. Scheme I and Table I show that a catalytic residue of $pK = 8.55$ acts as a proton donor in PPA. However, we cannot determine the residue that acts as a proton acceptor because of the small difference between the values of pK_1 and pK_2. The amino acid sequences at the active site of PPA and TAA are quite similar, and the amino acid residues near the catalytic site of PPA are compared to the three-dimensional structure of TAA (Buisson et al., 1987; Matsuura et al., 1984). Comparison of TAA with PPA indicates that the three His residues (101, 201, and 299 in PPA) and three carboxyl residues (197, 233, and 300 in PPA) are close enough to form hydrogen-bonding pairs. The enthalpy changes of the pK's and the information of the three-dimensional structure strongly suggest that the residues with pK values of 4.9 and 5.35 are carboxylates (Asp 197 or 300), and His, Cys, and Tyr are candidates for the residue with the pK value of 8.55. However, the most probable residue is His, since Cys and Tyr residues are probably not located in the catalytic site of PPA (Buisson et al., 1987).

PPA whose five His residues were modified chemically by diethyl pyrocarbonate at pH 6.0 (Nakatani, 1988; Ishikawa et al., 1989) showed a decrease in amylase activity and an increase in maltosidase activity. If the catalytic residue with the pK value of 8.55 is His, it cannot be modified by the reagent, since the chemical modification reagent is specific for the deprotonated His residue at pH 6.0; normal His residues (pK = 6–7) can be modified but the catalytic one with pK = 8.55 must be practically unmodified at pH 6.0. Therefore, steric hindrance around the His residue (one of the catalytic residues) may reduce the reactivity with the modification reagent.

The optimum pH of PPA for soluble starch shifted from 6.9 to 5.5 when the chloride ion bound to PPA was eliminated, although the enzyme activity was much lowered (Wakim et al., 1969). Therefore, chloride ion also affects the relative values of the two parameters k_1 and k_2 in Scheme I. Since the chloride ion binding site is near the active site (Buisson et al., 1987), far from subsite 5, the molecular mechanism for the optimum pH shift due to the chloride ion may be different from that in the substrate effect; chloride ion binding is an additional indispensable factor for optimum pH being around 7. Drastic differences in the k_1 and k_2 values and the optimum pH's between maltopentaitol and maltopentaose (Figures 2 and 4) suggest that the binding modes are not the same despite the fact that the substrates are quite similar in structure.

Subtle differences in the end group of these substrates and of glucose and sorbitol, as well as the binding of chloride ion, have a pronounced influence on the catalytic mechanism.

TAA shows a simple bell-shaped pH profile with the optimum pH around 5.5, regardless of the character of substrates (Matsubara et al., 1959); its catalytic residues are composed of two carboxyl groups, a donor and an acceptor (Matsuura et al., 1984). The present data and analysis show that the catalytic function of PPA consists of at least three ionizable residues. Previously proposed catalytic mechanisms that assume only two catalytic residues (Thoma, 1968; Buisson et al., 1987) should be extended so as to include an additional modulation factor. The residue of pK_3 acting as a proton donor is His, and the other two residues of pK_{1-2} are probably carboxyl residues acting as a proton acceptor and its modulator. Therefore, the catalytic mechanism of PPA should be constructed including an additional modulation mode to distinguish characters of substrates in the productive binding mode by protonation and deprotonation of the probable carboxyl residue at the active site. Our data and X-ray structure suggest that the proton donor for the catalysis of PPA is a His residue, either His 101, 201, and 299, and the active carboxyl residues are two of the three residues Asp 197, Glu 233, and Asp 300. To clarify the detailed catalytic mechanism of PPA, further structural and biochemical investigations are necessary.

Furthermore, it has been found that binding of a glucose residue to subsite 5 in the productive binding mode affects the transition state of hydrolysis at the catalytic site (Figure 5). It is reasonable to assume that the interaction between each subsite and a glucose residue in the enzyme–substrate complex is not rigid and not independent in PPA but flexible, especially at subsites 3 and 4, in which the catalytic site is located. The productive binding mode covering subsite 5 with a glucose residue must change configurations between the catalytic residues and the glycosidic bond hydrolyzed. If some pentamer substrates containing glucose analogues at the reducing end are used for pH profile determination, more information will be obtained about relationships between the binding site and the catalytic site.

References

Abdullah, M., French, D., & Robyt, J. F. (1966) *Arch. Biochem. Biophys. 114*, 595–598.

Buisson, G., Duee, E., Haser, R., & Payan, F. (1987) *EMBO J. 6*, 3909–3916.

Davis, B. J. (1964) *Ann. N.Y. Acad. Sci. 121*, 407–427.

Dixon, M., Webb, E., Thorne, C. J. R., & Tipton, K. F. (1979) *Enzymes*, pp 138–164, Academic Press, New York and San Francisco.

Dygert, S., Li, L. H., & Thoma, J. A. (1965) *Anal. Biochem. 13*, 367–374.

Elodi, P. (1972) *Acta Biochim. Biophys. Acad. Sci. Hung. 7*, 241–245.

Elodi, P., Mora, S., & Kryzteva, M. (1972) *Eur. J. Biochem. 24*, 572–581.

Hiromi, K., Takahashi, Y., & Ono S. (1963) *Bull. Chem. Soc. Jpn. 36*, 563–569.

Hoschke, A., Laszlo, E., & Hollo, J. (1980) *Carbohydr. Res. 81*, 145–156.

Ishikawa, K., & Hirata, H. (1989) *Arch. Biochem. Biophys. 272*, 356–363.

Kluh, I. (1981) *FEBS Lett. 136*, 231–234.

Kondo, H., Nakatani, H., & Hiromi, K. (1976) *J. Biochem. (Tokyo) 79*, 393–405.

Kondo, H., Nakatani, H., Hiromi, K., & Matuno, R. (1978) *J. Biochem. (Tokyo) 84*, 403–417.

Levitzki, A., & Steer, M. L. (1974) *Eur. J. Biochem. 41*, 171–180.

Loyter, A., & Shramm, M. (1962) *Biochim. Biophys. Acta 65*, 200–206.

Marchis-Mouren, G., & Pasero, L. (1967) *Biochim. Biophys. Acta 140*, 366–368.

Matsubara, S., Ikenaka, T., & Akabori, S. (1959) *J. Biochem. (Tokyo) 46*, 425–431.

Matsuura, Y., Kusunoki, M., Harada, W., & Kakudo, M. (1984) *J. Biochem. (Tokyo) 95*, 697–702.

Nakagawa, T., & Oyanagi, Y. (1980) Program System SALS for Nonlinear Least-Squares Fitting in Experimental Sciences, in *Recent Developments in Statistical Inference and Data Analysis* (Matusita, K., Ed.) pp 221–225, North Holland Publishing Co., Amsterdam, The Netherlands.

Nakatani, H. (1988) *Arch. Biochem. Biophys. 263*, 364–368.

Pasero, L., Abadie, B., Chicheportiche, Y., Mazzei, Y., Moinier, D., Bizzozero, J. P., Fougereau, M., & Marchis-Mouren, G. (1981) *Biochimie 63*, 71–79.

Pasero, L., Mazzei-Pierron, Y., Abadie, B., Chicheportiche, Y., & Marchis-Mouren, G. (1986) *Biochim. Biophys. Acta 869*, 147–157.

Prodanov, E., Seigner, C., & Marchis-Mouren, G. (1984) *Biochem. Biophys. Res. Commun. 122*, 75–81.

Robyt, J. F., & French, D. (1967) *Arch. Biochem. Biophys. 122*, 8–16.

Robyt, J. F., & French, D. (1970a) *J. Biol. Chem. 45*, 3917–3927.

Robyt, J. F., & French, D. (1970b) *Arch. Biochem. Biophys. 138*, 622–670.

Sakano, Y., Takahashi, S., & Kobayashi, T. (1983) *J. Jpn. Soc. Starch Sci. 30*, 30–37.

Sakoda, M., & Hiromi, K. (1976) *J. Biochem. (Tokyo) 80*, 547–555.

Thoma, J. A. (1968) *J. Theor. Biol. 19*, 297–310

Wakim, J., Robinson, M., & Thoma, J. A. (1969) *Carbohydr. Res. 10*, 487–503.

Walform, M. L., & Thompson, A. (1963) *Methods Carbohydr. Chem. 2*, 65–68.